# THE INFLUENCE OF SMALL TUBE DIAMETER AND INCLINATION ANGLE ON FLOODING PHENOMENA

*A.A. Mouza, S.V. Paras and A.J. Karabelas\**

Department of Chemical Engineering
and Chemical Process Engineering Research Institute
Aristotle University of Thessaloniki
Univ. Box 455, GR 540 06  Thessaloniki, GREECE
\* *tel*: 30-31-0996201    *e-mail*: karabaj@cperi.certh.gr

**Abstract**

This work is focused on flooding in small diameter tubes and presents new data on the effect of tube diameter, inclination angle and liquid properties on the mechanisms triggering flooding. Experiments are carried out with four relatively small i.d. tubes (i.e. 6, 7, 8 and 9mm) with smooth inlet and outlet conditions for air and two liquids (water and kerosene), in the range of inclination angles 30 to 90 deg. Experimental data on free flowing film characteristics have also been obtained, in the same test sections, which aid the interpretation of flooding phenomena. These new data suggest that the tube diameter strongly affects film flow development, especially in vertical tubes, apparently promoting wave interaction and damping. For inclined tubes the effect of tube i.d. and angle of inclination on gas flooding velocity is significant. In both vertical and inclined tubes, the influence of liquid physical properties is most pronounced. The trend of critical flooding velocity, under various conditions, is discussed in terms of possible mechanisms resulting from the aforementioned effects. Tentative correlations are also presented, useful for practical applications.

**INTRODUCTION**

In recent years there is considerable interest in understanding flooding of narrow flow passages, stemming mainly from efforts to develop compact devices such as plate heat exchangers and condensers made of corrugated plates. Typical flow passages therein are characterized by equivalent diameters of order 10 mm; consequently, counter-current gas/liquid flow in *small diameter* tubes may be considered an essential element of the complicated flow field of a compact reflux condenser, usually made of corrugated plates. It must be noted that, although flooding has been extensively studied in recent decades, there is still a great deal of uncertainty concerning the prevailing mechanisms as well as the most appropriate correlations for practical applications.

Flooding in **small diameter tubes** (in the **vertical** or **inclined** position) has received inadequate attention. Review papers (e.g. Bankoff & Lee, 1986 and Hewitt, 1995) provide a good account of information on flooding, which deals mainly with experiments in *vertical* tubes with i.d. much larger than the sizes considered here. As regards inclined tubes, the limited flooding data reported concern tubes with diameters greater than 20mm (e.g. Barnea et al., 1986; Celata et al., 1992; Zapke & Kroeger, 1996; Wongwises, 1998). In general, the factors that tend to influence the onset of flooding (e.g. Hewitt 1995; Zapke & Kroeger, 1996) are the conduit dimensions, the type of liquid and gas entry, the liquid properties and the inclination angle. There is evidence that the critical flooding velocity tends to decrease with increasing liquid viscosity (e.g. Clift et al., 1966) and decreasing surface tension (e.g. Zapke & Kroeger, 2000b).

The most widely used correlation for the flooding limit (although quite often unsuccessfully, Bankoff & Lee (1986)) is due to Wallis (1969), which was developed for *vertical* tubes and does not take into consideration the effect of fluid properties (i.e. viscosity, surface tension):

$$\sqrt{U_G^*} + C_1 \sqrt{U_L^*} = C_2 \qquad (1)$$

where $U_{G,L}^* = U_{GS,LS} \sqrt{\dfrac{\rho_{G,L}}{gD(\rho_L - \rho_G)}}$ is a dimensionless velocity with $U_{GS}$ and $U_{LS}$ the superficial gas and liquid velocities respectively, $\rho_G$ and $\rho_L$ the phase densities, $g$ the acceleration due to gravity and $D$ the tube inside diameter. The parameters $C_1 = 0.8$ -1.0 and $C_2 = 0.7 - 1.0$, depend mainly on geometry. Many efforts have been made over the years to

improve the Wallis correlation by dealing with the coefficients $C_1$, $C_2$ and by introducing various dimensionless numbers to account for the observed effects of liquid properties. For example, Zapke & Kroeger (1996) employ a modified version of the Wallis expression, where the effect of the fluid properties, the tube inclination and gas inlet configuration on flooding, is also incorporated, as follows:

$$\sqrt{U_G^*} + m\sqrt{U_L^*} = EZ_L^b \tag{2}$$

where $Z_L = \dfrac{\sqrt{D\rho_L\sigma}}{\mu_L}$ is the inverse *Ohnesorge* number, with $\rho_L$, $\mu_L$, $\sigma$ the properties of the liquid phase and *b, E* and *m* designate empirical constants that depend on tube inclination angle and tube-end configuration. ***Eqs (1)*** and ***(2)*** imply that there is a linear relationship between $\sqrt{U_L^*}$ and $\sqrt{U_G^*}$. ***Eq. (2)*** was tested for various liquids with a fairly broad range of viscosity (0.57-2.5 x10$^{-3}$ kg/ms) and surface tension (23-72 x10$^{-3}$ N/m). However, as the experiments were conducted with only one tube i.d., its validity for other (especially smaller) diameters is still untested.

There has been considerable debate in the past concerning the dominant mechanisms of flooding:

- In ***vertical tubes*** there appears to be an agreement (Hewitt, 1995; Jayanti et al., 1996) that flooding is brought about by two types of gross mechanisms, i.e. upward transport of waves mainly from the area close to liquid outlet, and carryover of droplets from disintegration of the falling liquid film. The former mechanism seems to dominate in relatively small diameter tubes (where the total drag exerted by the gas on waves can overcome the gravity force), whereas the latter is evident in relatively large i.d. tubes and is associated with higher flooding velocities. It will be pointed out here that the experimental evidence that helped identify these trends, was obtained with tube diameters much larger than those considered in the present study. Recognizing that the cause of flooding resides in the complicated interaction of gas flow with a wavy liquid film interface, some theoretical attempts have been made to model flooding (e.g. Shearer & Davidson, 1965; Cetinbudaklar & Jameson, 1969; No & Jeong, 1996) based on liquid wave growth and stability analysis. The success of such efforts has been limited at best.

- In ***inclined tubes*** Barnea et al (1986), trying to elucidate the complicated effect of inclination angle on flooding in counter-current stratified flow, point out some (intuitively) counter acting trends with increasing angle of inclination; i.e. the decreasing thickness of faster flowing liquid layer, the increasing height of waves at the gas/liquid interface, and the increasing tendency for lateral wave spreading. They report, as a net effect, that the critical flooding velocity tends to "…increase and then decrease as the inclination angle is changed from horizontal to vertical…". However, this conclusion has not been verified by other studies.

In view of the aforementioned multitude of factors involved, and the uncertainty concerning the true mechanisms, it is not surprising that reliable predictive tools of general validity are not available at present, even for flooding in fairly large diameter vertical pipes.

In efforts to model flooding, quite often the characteristics of free falling films (in the absence of air flow) are invoked and utilized. A significant experimental observation (partly justifying this choice) is the fact (e.g. Nickling & Davidson, 1962; Zabaras & Dukler, 1988; Dukler et al., 1984) that the mean liquid film thickness (estimated by the Nusselt expression) remains essentially unaffected by the counter-current gas flow almost up to the critical flooding conditions. Therefore, it may be advantageous to use relevant information on wavy free falling films in order to clarify incipient flooding. Systematically obtained falling film data for flow inside ***small*** i.d. tubes are not available in the literature, to the authors' knowledge.

Motivated by the above considerations this work is focused on flooding in small diameter tubes. Data on free falling liquid films are also obtained (both in vertical and inclined geometries) as part of the effort to clarify the influence of the liquid film characteristics on flooding phenomena. Additionally appropriate analytical expressions for the prediction of the liquid film thickness in vertical and inclined tubes were developed and checked.

## EXPERIMENTAL SETUP

Flooding experiments have been carried out in vertical and inclined (inclination angle 30 to 90 deg from horizontal) small i.d. tubes (6, 7, 8 and 9 mm), using smooth inlet and outlet conditions, with air and two liquids (water and kerosene) (***Figure 1***). The test sections are made of glass. Air enters at the bottom through a small tube, while the liquid is introduced

uniformly at the top, through a specially machined porous wall segment. The physical properties of the fluids used are included in **Table 1**.

Table 1. Physical properties of fluids.

|  | kerosene | water | air |
|---|---|---|---|
| Density, $\rho$, kg/m$^3$ | 800 | 1000 | 1.2 |
| Viscosity, $\mu$, kg/m.s | $1.4 \times 10^{-3}$ | $1.0 \times 10^{-3}$ | $1.8 \times 10^{-5}$ |
| Surface tension, $\sigma$, kg/sec$^2$ | 0.028 | 0.072 | - |

Observations are made using a high-speed camera (*Redlake MotionScope PCI*®) in order to identify the basic mechanisms triggering flooding. The imaging system used is capable of recording up to 1000 full frames per second, but in the present experiments pictures are taken at a speed of 250 frames per second and a shutter rate of 1/1000 at three different locations along the pipe, i.e. just below the liquid entrance, at the liquid exit, and at an intermediate location. The film trace at a point along the tube is measured using an optical method. The characteristics of the film (e.g. mean thickness, RMS, wave height) are obtained by statistical methods. Details of the method are presented elsewhere (Mouza et al., 2002a).
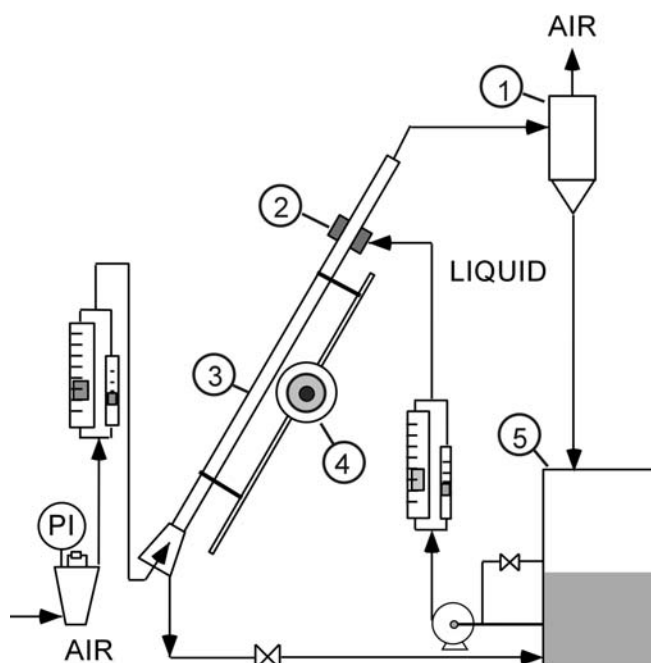


Figure 1. Experimental flow loop:1. Phase separator; 2. Porous wall section; 3. Glass test tube; 4. Rotating support; 5. Liquid storage tank

**RESULTS**

In ***Figure 2*** typical results for the 7mm i.d. tube are presented (for water and kerosene), where the critical gas velocity $U_{GS}$ necessary for incipient flooding is plotted against the corresponding liquid Reynolds number, $\mathrm{Re}_{LS} = \dfrac{U_{LS}D}{\nu_L}$, where $\nu_L$ is the liquid kinematic viscosity. For the various experimental runs the designation ***FD_φ*** is used, where *F*=w,k stands for water and kerosene, respectively; *D*=tube inside diameter [mm]; *φ*=inclination angle, deg from horizontal.

A general remark is that flooding is initiated at lower velocities when kerosene is used, since the lower surface tension of kerosene favors the formation of waves. The data show that the influence of the ***inclination angle*** is strong and the flooding velocity is considerably smaller at the vertical position. The flow pattern before flooding is different in vertical tubes than in the inclined ones, and therefore the two cases are considered separately. In all cases ***three*** distinct regions can be readily observed (as marked in ***Figure 2a***).

**Vertical tubes**

At small liquid Reynolds numbers i.e. in ***Region A*** (*Re$_{LS}$*<200-300) critical flooding velocities, $U_{GS}$, follow a trend already reported in the literature, i.e. decreasing with increasing liquid rate. The visual observations reveal that in this region coherent waves grow on the falling film moving towards the liquid exit. The motion of one of these large waves may be "arrested" by the counter-current gas flow leading to its rapid growth until the drag force exerted by the gas is large enough to overcome the gravity force and transport it upwards. Therefore, the flooding mechanism is the upward transport of a solitary wave, a trend observed mainly in the smaller diameter pipes, where the gas flow area reduction due to waves is large (Jayanti et al.,1996). The flooding velocity may be predicted by assuming that flooding is initiated when the drag forces counterbalance the gravity forces. For this reason, the forces exerted on a standing wave were calculated using a commercial CFD code (CFX®). Two consecutive photos of a wave arrested at the liquid exit (***Figure 3a***) were digitized (***Figure 3b***) and their shapes were introduced in the CFX® code and used to construct the gas phase "conduit" (***Figure 3c***).

The first photo corresponds to the moment when the motion of the wave is arrested (t=0) whereas the second corresponds to a wave just before incipient flooding (Δt=12ms). The total drag force exerted on the "frozen" wave is calculated for a number of gas velocities

for both wave profiles. The calculations show that for the first wave (t=0) the drag force does not counterbalance the gravity force even for high mean gas velocities. On the contrary for the second wave (t=12ms) the drag force tends to overcome the gravity forces for a gas velocity $U_G$=5.8m/s, which is in fair agreement with the experimental value of 5.2m/s.

The mechanism prevailing in Region A has already been described by several researchers (e.g. Hewitt, 1995) and the new data for the small diameters follow a Wallis type correlation (*Figure 4*).
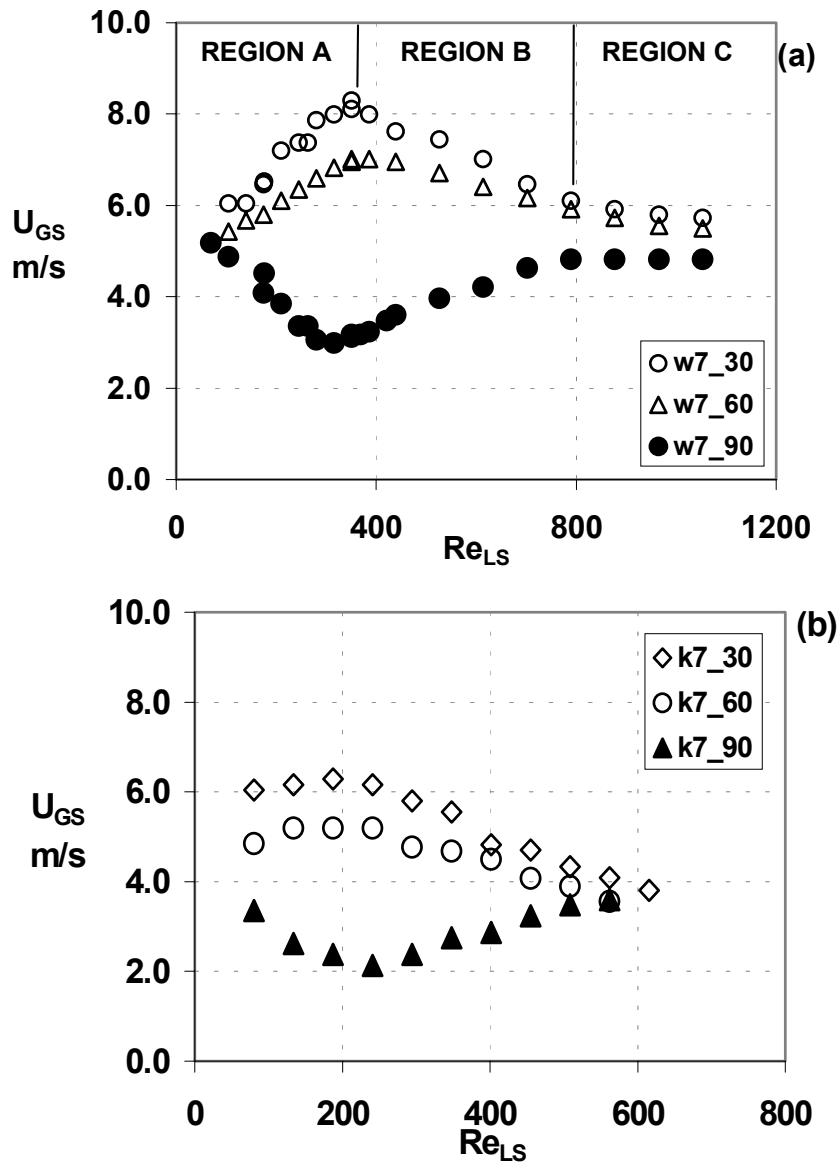


Figure 2. Critical gas flooding velocities versus liquid Reynolds number. Effect of inclination angle in a 7mm tube; (a) water (b) kerosene
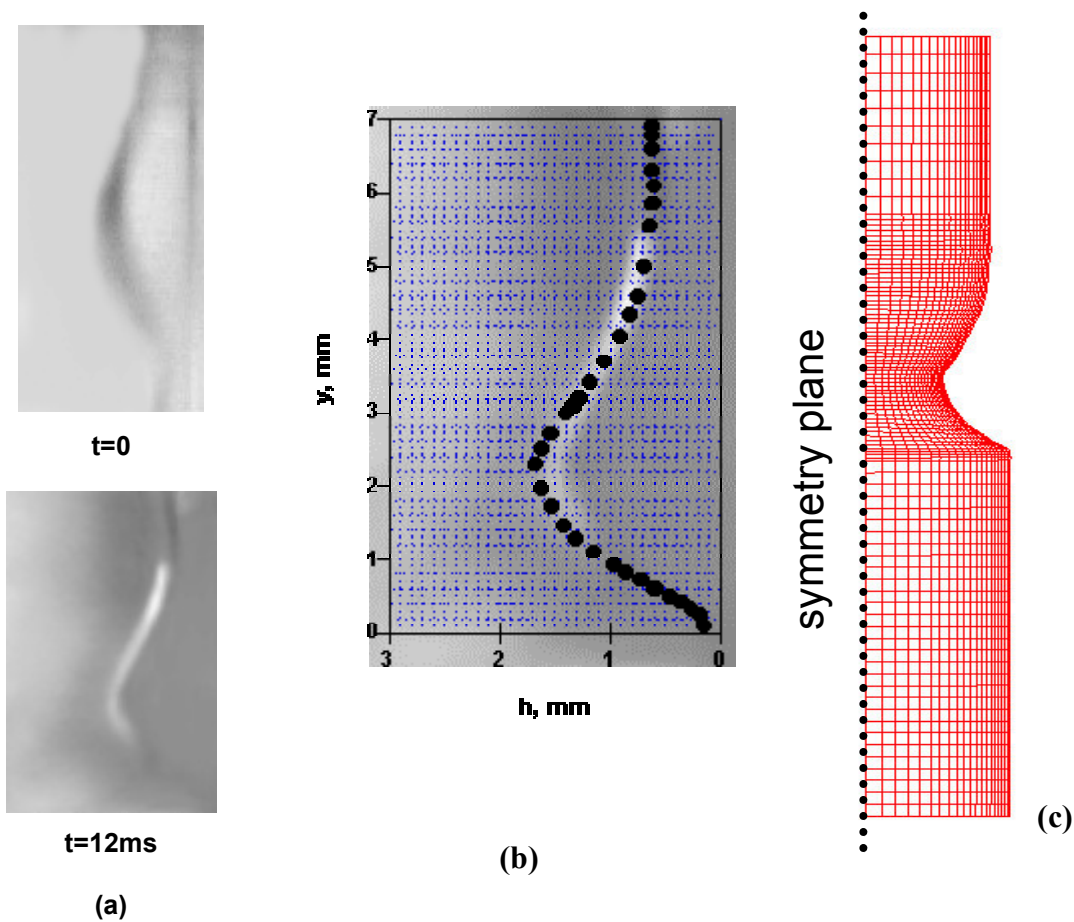
Figure 3. Construction of the gas phase "conduit" for the CFD simulation.
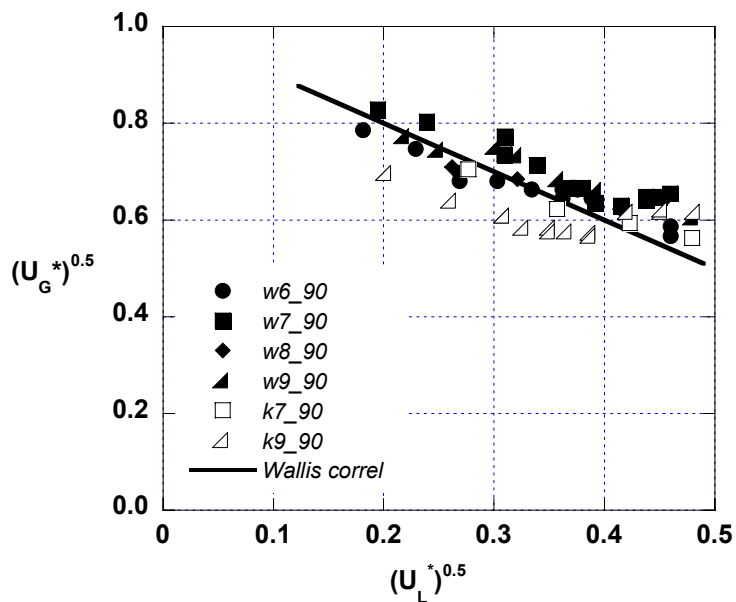


Figure 4. Comparison of experimental data with the Wallis correlation of the form:

$$\sqrt{U_L^*} + \sqrt{U_G^*} = 1.$$

8

At higher $Re_{LS}$ (**Region B**) the trend is reversed, i.e. increasing $U_{GS}$ with increasing liquid rate. The extent of this region is reduced as the tube diameter increases and tends to disappear for the larger tube diameters (i.e. 9mm) (**Figure 5**). This trend has not been reported in the literature before and may be attributed to *damping of waves*. This region is less pronounced when the lower surface tension kerosene is used.

New experimental data on free falling film characteristics in the same test sections (Mouza et al., 2002a) suggest that the tube diameter strongly affects film flow development; furthermore, the wavy film evolution essentially determines flooding characteristics. It appears that in small diameter tubes (i.d.<10mm) the curvature plays a significant role in the mechanism by which flooding occurs; it influences wave evolution by hindering the unrestricted lateral growth of waves and by promoting wave interaction and damping. It must be added that even the smallest deviation from the vertical position changes drastically the flooding mechanisms observed.

At still higher $Re_{LS}$, another region (**Region C**) is clearly evident in the flooding curves, characterized by nearly constant flooding velocity, that exhibits a rather strong dependence on tube diameter, and (quite unexpectedly) it is generally greater for the smaller diameter tubes. Depending on the tube diameter, two different mechanisms are observed to be responsible for the onset of flooding. In the 8 and 9mm tubes for both liquids tested, a finite amplitude wave formed close to the liquid exit rapidly grows and **chokes** the flow. The liquid is then pushed up as a liquid **slug** or as a mixed **entrained** phase. A different mechanism prevails in tube i.d.≤7mm, where the falling film pictures reveal that the waves are not coherent. In this case flooding occurs due to blockage just below the liquid entrance, but at fairly high gas velocities. It is speculated that the cause of **entrance** flooding at these high liquid rates is the thickening of the liquid film at the entrance porous section.

To assist data interpretation, an analytical expression has been developed for the prediction of the film thickness, $h_o$, corresponding to a fully developed laminar free falling film, flowing *inside small diameter tubes*. The value of $h_o$ obtained from this expression is more representative of the problem treated here than the well-known *Nusselt* mean film thickness, which corresponds to flow on a flat surface and is, therefore, independent of tube diameter.
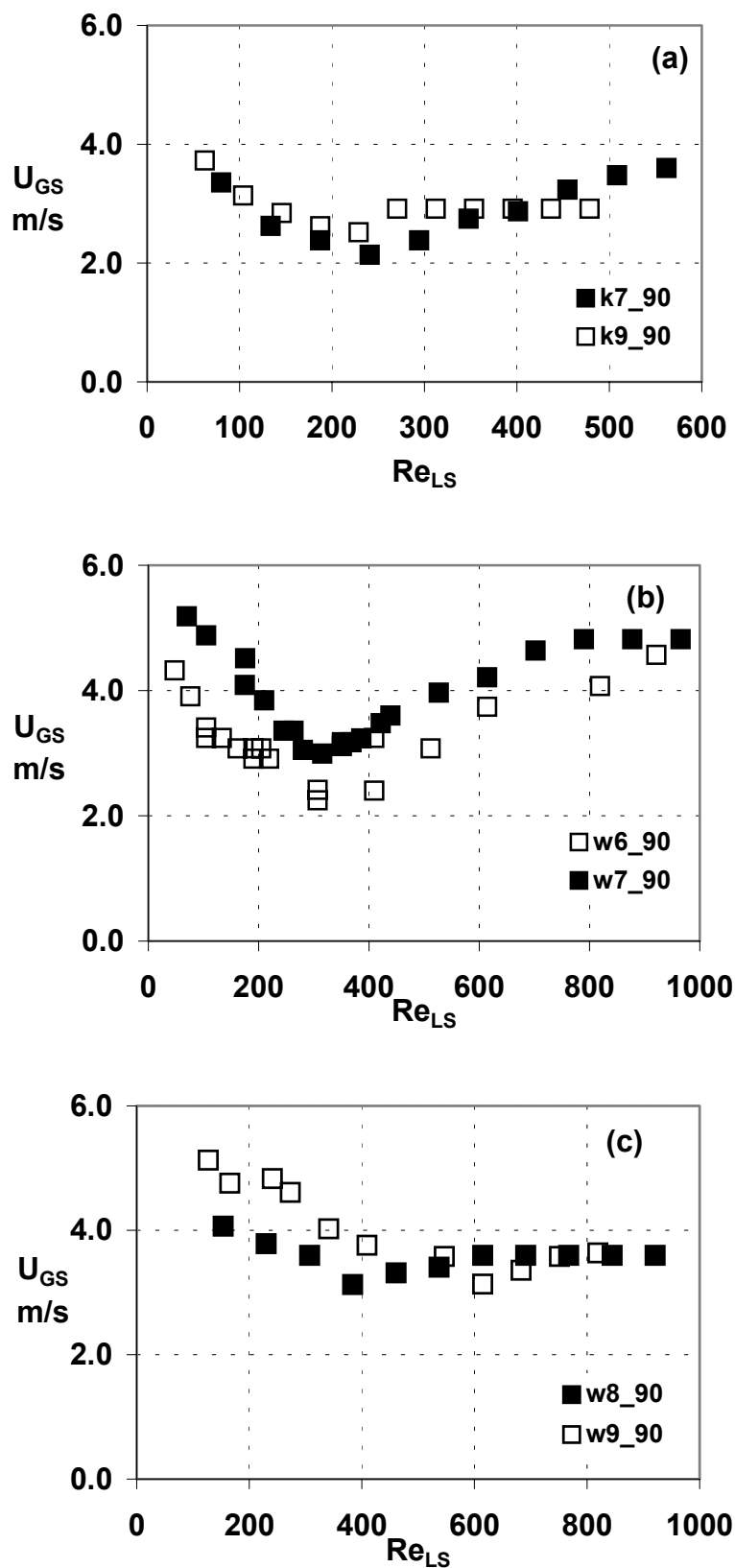
9

Figure 5. Critical gas flooding velocities versus liquid Reynolds number; (a) kerosene; (b) water in 6mm and 7mm i.d. tubes; (c) water in 8mm and 9mm tubes.

The film thickness, $h_o$, is obtained from the following expression:

$$Q = \frac{\pi \rho g R^4}{8\mu}\left[\left(1 - \lambda^2\right)\left(1 - 3\lambda^2\right) - 4\lambda^4 \ln\lambda\right]$$ (3)

where Q is the liquid volumetric flow rate, $R$ is the tube inside radius and $\lambda = \dfrac{R - h_o}{R}$. *Figure 6* presents the variation of mean film thickness with liquid Reynolds number for 7 and 9mm i.d. tubes. There is fair agreement of experimentally determined values of mean film thickness with the theoretical ones for smooth laminar films, predicted by means of *Eq. (3)*.

To take into account the effect of fluid properties and conduit dimensions a correlation is presented by using gas/liquid *Froude* numbers and the *Bond* number. In *Figure 7* the data are plotted in terms of gas Froude number based on superficial gas velocity, at incipient flooding, versus the ratio of the corresponding liquid *Froude* number over the *Bond* number, where the Froude and Bond numbers are defined as:

$$Fr_{L,G} = U_{L,G}^2 \rho_{L,G} / g D\left(\rho_L - \rho_G\right)$$ (4)

$$Bo = D^2 g\left(\rho_L - \rho_G\right)/\sigma$$ (5)

The data are brought together reasonably well. It is noteworthy that the transition from Region A to B takes place at a constant value of the quantity $(Fr_L/Bo)^{0.5} = 0.06$ regardless of type of liquid and tube size employed in this study.
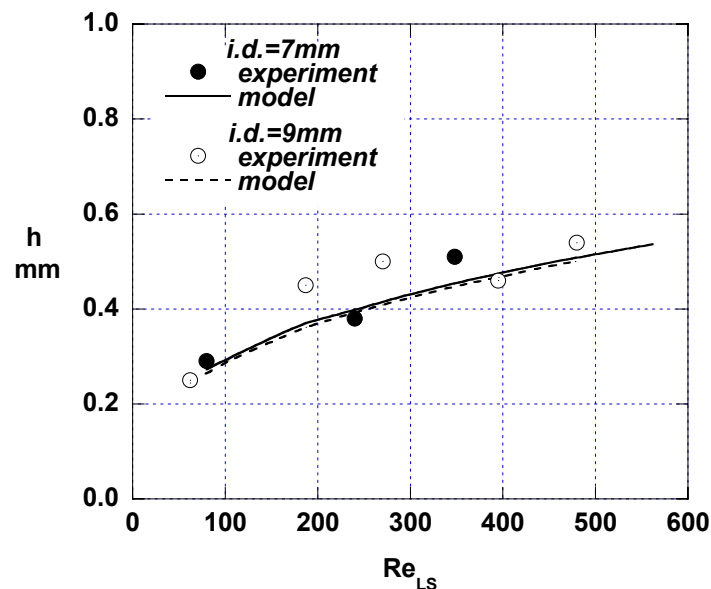


Figure 6. Mean free falling film thickness versus liquid Reynolds number; comparison of experimentally determined thickness with prediction (Mouza et al., 2002).
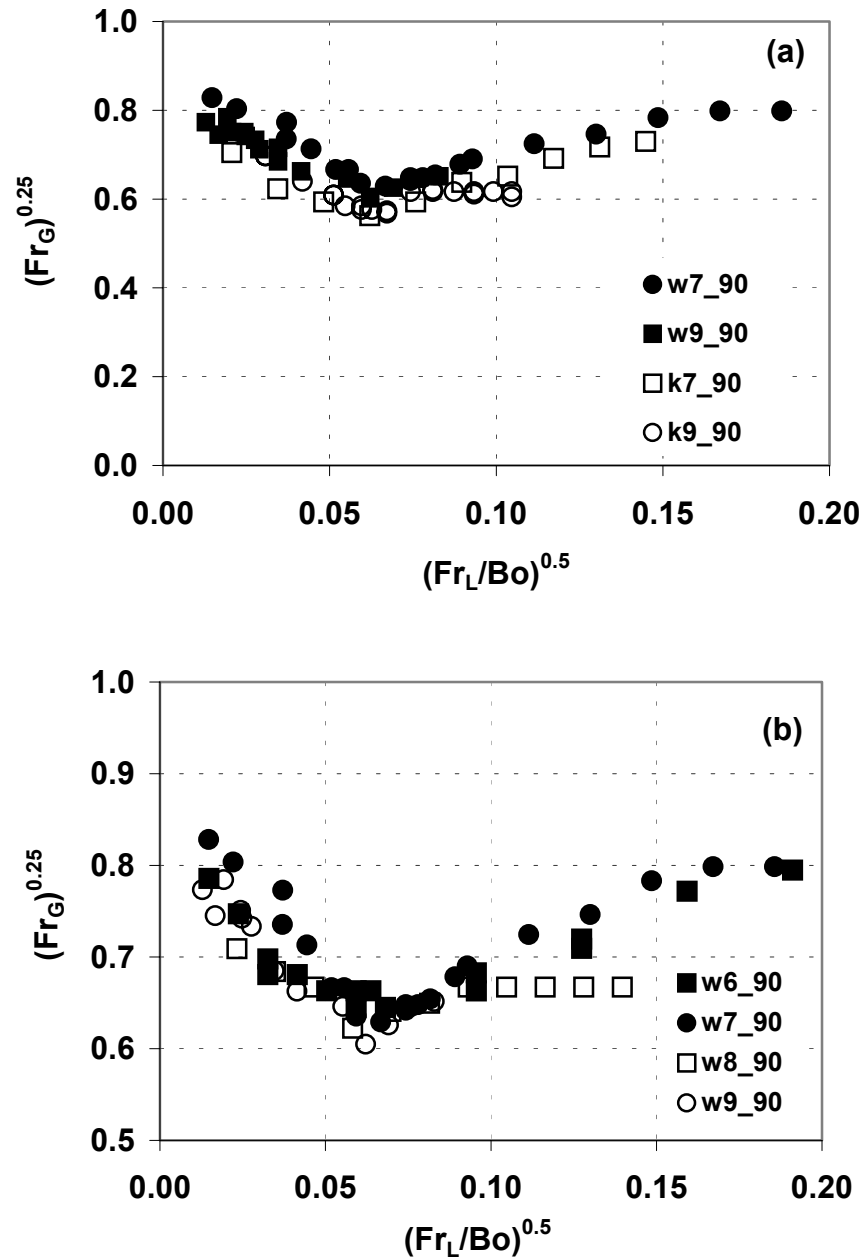
11

Figure 7. Critical gas Froude number versus the ratio of liquid Froude to Bond number. Typical curves for (a) water and kerosene; (b) water.

**Inclined tubes**

As shown in Figure 2, for the lower liquid flow rates tested (***Region A***) the critical $U_{GS}$ is roughly proportional to liquid rate, something not reported in the literature up to now. One may hypothesize that, in this range of small liquid rates with high tube curvature (i.e. in small i.d. tubes) lateral liquid spreading readily takes place, effectively reducing the amplitude of waves especially near the liquid exit where the onset of liquid flow reversal is observed. Thus, in this small-$Re_{LS}$ range, considering that the wave shape does not change significantly with

12

increasing liquid rate, an increased gas velocity would be required to generate high enough drag on the waves to counterbalance gravitational forces and reverse wave motion. The visually observed fairly symmetrical "ring"-type waves, moving upwards with the gas, tend to support this argument applying to Region A.

For larger liquid flow rates (***Region B***) the gas flooding velocity is roughly inversely proportional to the liquid superficial velocity, a trend well-known in the literature. In this region, the thicker and faster moving layer at the tube bottom would tend to favor the formation of 3-D waves (with reduced lateral spreading), which would grow and reverse their flow direction but at progressively smaller gas velocities. Visual observations suggest that this picture is typical of incipient flow reversal in Region B.

Visual observations suggest that, almost up to the critical gas flooding velocity, small amplitude waves exist on the liquid surface and the mean liquid layer thickness may not differ significantly from that of the free flowing layer in the absence of gas flow. Thus, the free flowing liquid thickness was measured in the absence of gas flow and for the liquid flow rates employed. Moreover, the visual observations reveal that, the film surface appears to be smooth and undisturbed. Thus, considering a flat and smooth interface, the thickness of a laminar free-flowing layer may be also estimated by an approximate analytical solution to the respective problem. For given liquid flow rate, tube diameter, inclination angle as well as liquid density and viscosity, the free flowing liquid layer thickness can be obtained (Mouza et al., 2002b).

In ***Figure 8*** a comparison of measured free flowing liquid layer thickness, $h$, with theoretical predictions for two tube diameters (i.e. 7 & 9mm) and two inclination angles (i.e. 30 & 60 deg from horizontal) is presented. The measured values are in fair agreement with the predictions.

From the visual observations and careful inspection of the experimental results (***Figures 2*** and ***9***) it can be concluded that the gas velocity necessary to cause incipient flooding is the outcome of the interaction of several parameters, the most important of which are:

- the physical properties of the liquid phase (surface tension and viscosity),
- the liquid layer velocity,
- the tube diameter and
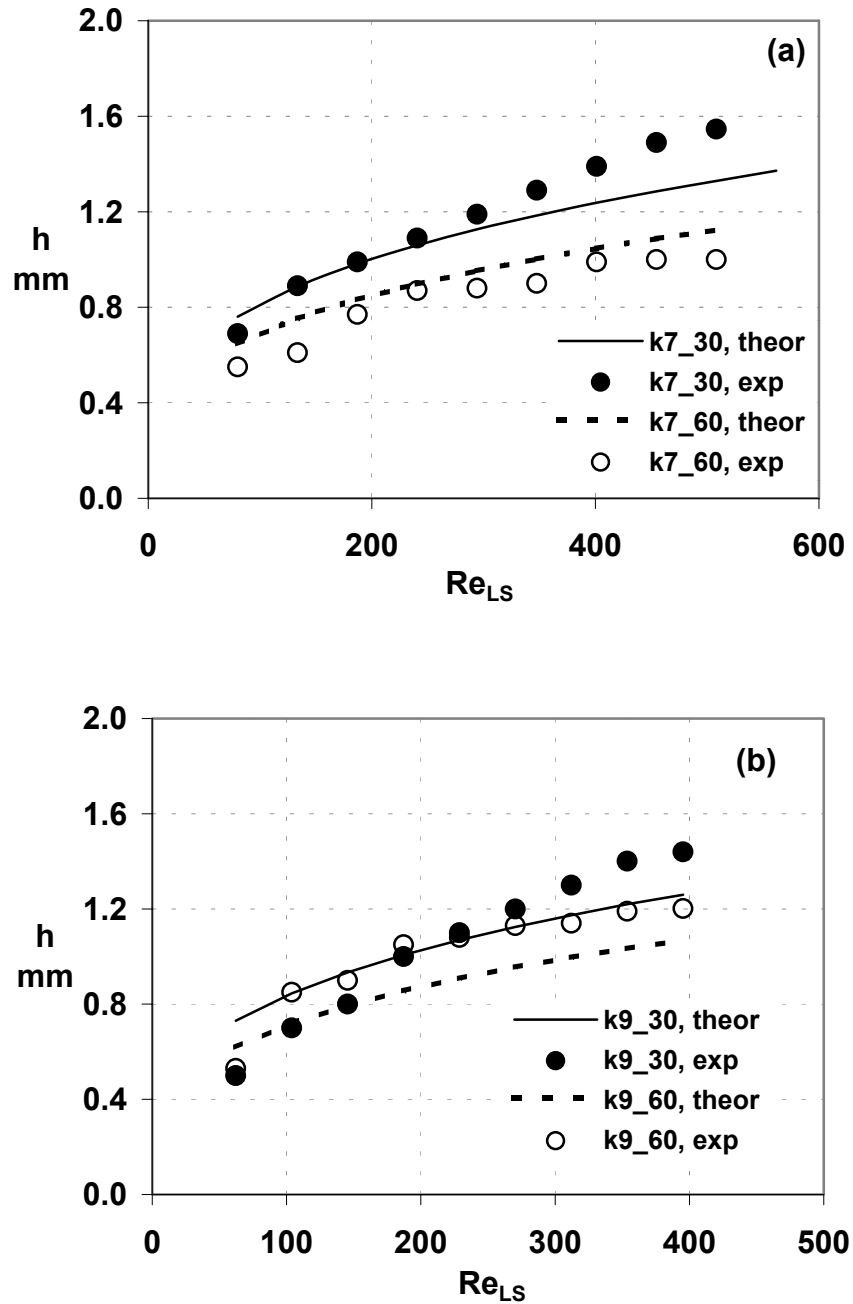- the tube inclination angle.

Figure 8. Comparison of measured free flowing liquid layer thickness, *h*, with theoretical predictions (Mouza et al., 2002b) for two inclination angles: a) *i.d.*=7mm and b) *i.d.*=9mm.

An attempt is made to develop a correlation to take into account these parameters, by defining an appropriate liquid Froude number, $Fr_{LH}$, gas Reynolds number, $Re_{GH}$ and liquid Kapitsa number, $Ka$:

$$Fr_{LH} = \frac{\langle U_L \rangle^2}{D_{LH}\, g \sin\varphi} \ , \ \mathrm{Re}_{GH} = \frac{\langle U_G \rangle D_{GH}}{\nu_G}, \ Ka = \frac{\sigma_L}{\left(\nu_L\, g \sin\varphi\right)^{1/3} \mu_L}$$

14

where $\langle U_{L,G} \rangle = Q_{L,G}/A_{L,G}$ the mean phase velocity, $A_{L,G}$ the cross sections of the liquid and gas phase "conduits", $D_{LH,GH}$ hydraulic diameters of the liquid and gas phase "conduits" and $\varphi$ tube inclination angle (degrees from horizontal).
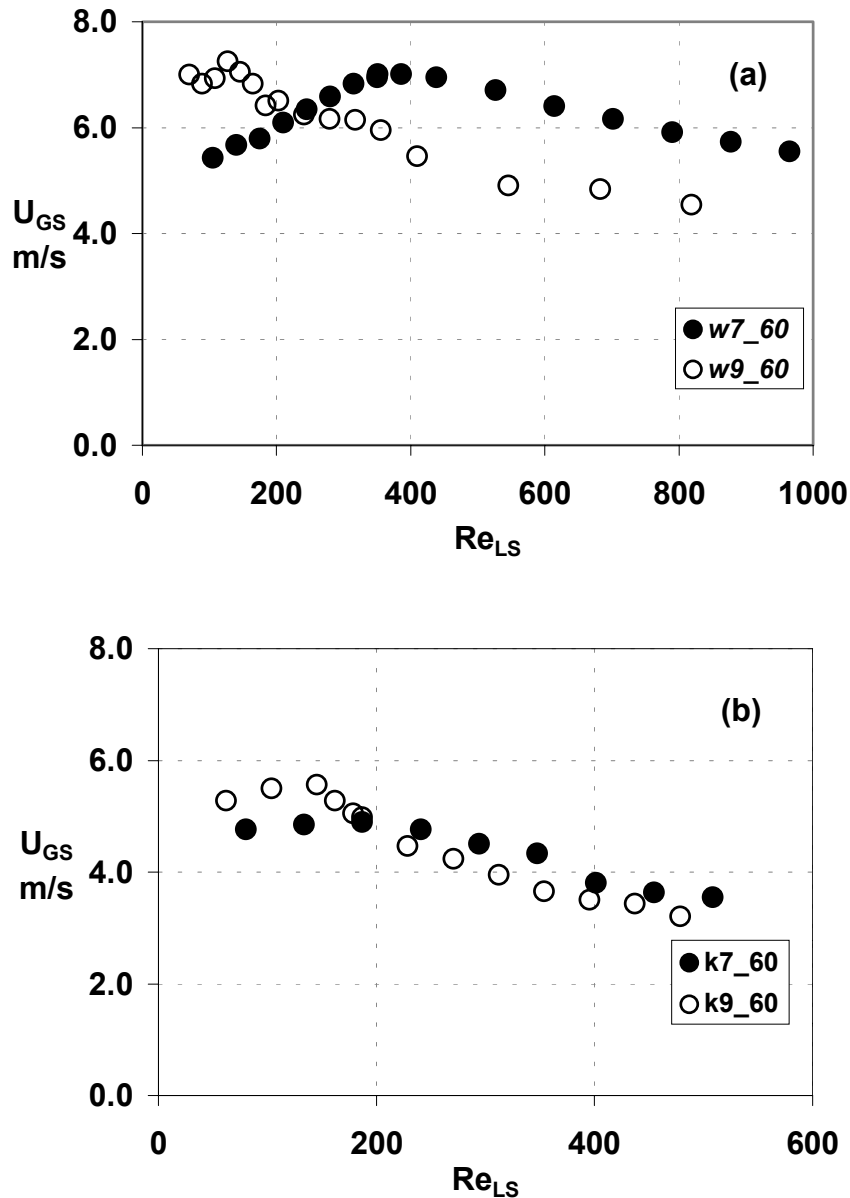


Figure 9. The superficial gas Reynolds number at incipient flooding versus the corresponding superficial liquid Reynolds number. Effect of tube diameter on the form of flooding curve: (a) water, (b) kerosene.

The liquid layer cross section, $A_L$, can be calculated from the tube diameter and the mean liquid layer thickness, $h$, which in turn can be predicted using the procedure suggested by Mouza et al. (2002b).

In **Figure 10** the quantity $\dfrac{\mathrm{Re}_{GH}}{Ka^{0.4}}$ at flooding point is plotted against the corresponding liquid Froude number, $Fr_{LH}$. It is evident that the data points (excluding those of Region A) tend to fall roughly along a line of the following form:

$$\frac{\mathrm{Re}_{GH}}{Ka^{0.4}} = aFr_{LH}^{-0.5} \tag{6}$$

This correlation appears to provide first estimates of (possibly a maximum) critical flooding velocity for relatively small viscosity fluids and small i.d. tubes. It is worth noting that this correlation is consistent essentially with all major dependencies of the critical gas velocity outlined above.
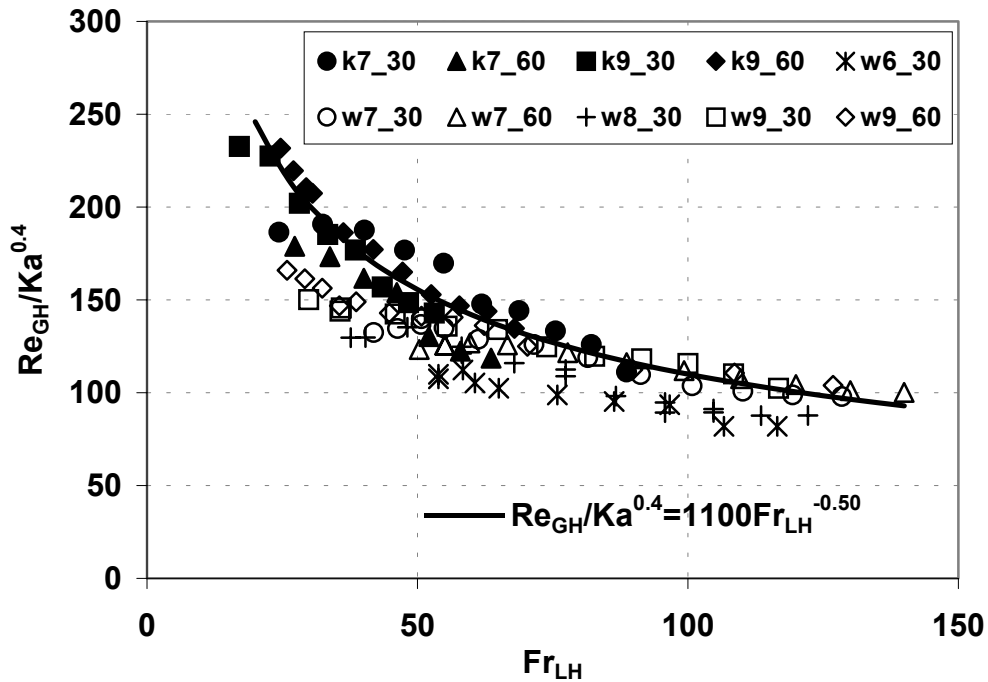


Figure 10. The quantity $\dfrac{\mathrm{Re}_{GH}}{Ka^{0.4}}$ at flooding point vs. the corresponding liquid Froude number, $Fr_{LH}$.

**CONCLUDING REMARKS**

Flooding in the low end of the liquid Reynolds number ($Re_{LS}$) range is investigated with relatively small i.d. tubes. Under these conditions, the effect of tube i.d., angle of inclination, $\varphi$, and of liquid physical properties on flooding is significant. It is interesting that the critical

flooding velocities in *vertical* ($\varphi=90^{o}$) tubes are significantly smaller than those corresponding to *inclined* tubes, all other conditions being the same. Moreover, a decreasing angle of inclination, $\varphi$, is associated with an increasing critical $U_{GS}$; this observation appears to be consistence with our physical intuition and useful for practical applications.

For *vertical* tubes and small $Re_L$ (Region A), the flooding velocity follows a Wallis-type correlation, i.e. decreasing with increasing liquid flow rate. From the viewpoint of practical application of results, it may be significant that beyond Region A (i.e. at relatively high $Re_{LS}$) the critical flooding velocity tends to increase. This trend is considered beneficial for operating compact condensers, as it may broaden their region of operability. An estimate of the transition Reynolds number (from Region A to B) for small i.d. tubes may be obtained from the expression $(Fr_L/Bo)^{0.5}\approx0.06$, although more data are required to test its reliability.

For the *inclined* tubes, an expression based on the dimensionless Kapitsa and liquid Froude numbers seems to be appropriate for correlating the new data, providing first estimates of the critical flooding velocity for small i.d. tubes, necessary for designing heat transfer equipment.

In closing, additional work is required to thoroughly comprehend film flow development and flooding phenomena in small i.d. tubes. More data are also needed to check the validity of the proposed correlations.

**REFERENCES**

Bankoff S.G. & Lee, S.C. 1986 A critical review of the flooding literature, in G.F. Hewitt, J.M. Delhaye and N. Zuber (ed.), *Multiphase Science and Technology*, vol. 2, chap. 2, Hemisphere Corp, N.Y.

Barnea, D, Ben Yosef, N. and Taitel, Y. 1986 Flooding in Inclined Pipes – Effect of Entrance Section., *The Can. J. of Chem. Eng.*, vol. 64, pp 177-184.

Celata, G.P., Cumo, M. & Setaro, T. 1992 Flooding in Inclined Pipes with Obstructions. *Exp. Thermal Fluid Science* **5**, 18-25

Cetinbudaklar, A.G. & Jameson, G.J. 1969 The mechanism of flooding in vertical countercurrent two-phase flow. *Chem. Eng. Sci.* **24**, 1669-1680.

Chang, H.C. 1994 Wave evolution on a falling film. Annu. Rev. Fluid Mech. 26, 103-136.

Clift, R., Pritchard, C.L. & Nederman, R.M. 1966 The effect of viscosity on the flooding conditions in wetted wall columns. *Chem. Eng. Sci*. **21**, 87-95

Dukler, A.E., Smith, L. and Chopra, A. 1984 Flooding and upward film flow in tubes-I Experimental studies. *Int. J. Multiphase Flow* **10**, 585-597.

Hewitt, G.F. 1995 In search of two-phase flow, Lecture, *30th US National Heat Transfer Conference*, Portland, Oregon.

Jayanti S., Tokarz A. and Hewitt, G.F. 1996 Theoretical investigation of the diameter effect on flooding in counter-current flow. *Int. J. Multiphase Flow* **22**, 307-324.

Mouza, A.A., Paras, S.V. & Karabelas, A.J. 2002a The influence of small tube diameter on falling film and flooding phenomena. *Int. J. Multiphase Flow* (accepted for publication).

Mouza, A.A., Paras, S.V. & Karabelas, A.J. 2002b Incipient flooding in inclined tubes of small diameter *Int. J. Multiphase Flow* (submitted for publication).

Nickling, D.J. and Davidson, J.F. 1962 The onset of instability in two phase slug flow. *Proc. I. Mech. Symp. Two-Phase Flow* London Feb. 1962 paper 7

No, H.C. and Jeong, J.H. 1996 Flooding correlation based on the concept of hyperbolicity breaking in a vertical annular flow. *Nuclear Engineering and Design* **166**, 249-258.

Shearer, C.J. and Davidson, J.F. 1965 The investigation of a standing wave due to gas blowing upwards over a liquid film; its relation to flooding in wetted-wall columns. *J. Fluid Mech.* **22**, 321-335.

Wallis, G.B. 1969 One-dimensional two-phase flow, McGraw-Hill, New York.

Wongwises, S. 1998 Effect of inclination angles and upper end conditions on the countercurrent flow limitation in straight circular pipes. *Int. Comm. Heat Mass Transfer*, **25**, 1, 117-125.

Zabaras, G.J. & Dukler, A.E. 1988 Countercurrent gas-liquid annular flow, including the flooding state. *AICHE J.* **34**, 389-396.

Zapke A. and Kroeger, D.G. 1996 The influence of fluid properties and inlet geometry on flooding in vertical and inclined tubes. *Int. J. Multiphase Flow* **22**, 461-472.

Zapke, A. and Kroeger, D.G. 2000a Counter-current gas-liquid flow in inclined and vertical ducts – I: Flow patterns, pressure drop characteristics and flooding. *Int. J. Multiphase Flow* **26**, 1439-1455.

Zapke, A. and Kroeger, D.G 2000b Counter-current gas-liquid flow in inclined and vertical ducts – II: The validity of the Froude-Ohnesorge number correlation for flooding. *Int. J. Multiphase Flow* **26**, 1457-1468.